AIP | Applied Physics Letters

Resistive switching in rectifying interfaces of metal-semiconductor-metal structures

R. Zazpe, P. Stoliar, F. Golmar, R. Llopis, F. Casanova et al.

Citation: Appl. Phys. Lett. **103**, 073114 (2013); doi: 10.1063/1.4818730
View online: http://dx.doi.org/10.1063/1.4818730
View Table of Contents: http://apl.aip.org/resource/1/APPLAB/v103/i7
Published by the AIP Publishing LLC.

Resistive switching in rectifying interfaces of metal-semiconductor-metal structures

R. Zazpe,[1] P. Stoliar,[1,2,3,a)] F. Golmar,[1,4] R. Llopis,[1] F. Casanova,[1,5] and L. E. Hueso[1,5]
[1]*CIC nanoGUNE, 20018 Donostia-San Sebastián, Basque Country, Spain*
[2]*IMN, Université de Nantes, CNRS, 2 rue de la Houssinière, BP 32229, 44322 Nantes, France*
[3]*ECyT, UNSAM, Martín de Irigoyen 3100, B1650JKA, San Martín, Bs As, Argentina*
[4]*I.N.T.I.–CONICET, Av. Gral. Paz 5445, Ed. 42, B1650JKA, San Martín, Bs As, Argentina*
[5]*IKERBASQUE, Basque Foundation for Science, 48011 Bilbao, Basque Country, Spain*

(Received 8 July 2013; accepted 30 July 2013; published online 15 August 2013)

We study the electrical characteristics of metal-semiconductor-metal HfO_{2-x}-based devices where both metal-semiconductor interfaces present bipolar resistive switching. The device exhibits an unusual current-voltage hysteresis loop that arises from the non-trivial interplay of the switching interfaces. We propose an experimental method to disentangle the individual characteristics of each interface based on hysteresis switching loops. A mathematical framework based on simple assumptions allows us to rationalize the whole behavior of the device and reproduce the experimental current-voltage curves of devices with different metallic contacts. We show that each interface complementarily switches between a nonlinear metal-semiconductor interface and an ohmic contact. © *2013 AIP Publishing LLC*. [http://dx.doi.org/10.1063/1.4818730]

Resistive random-access memories (ReRAM) are emerging as one of the most promising alternatives for the next generation of non-volatile electronic memories.[1–3] They are based on the resistive switching (RS) phenomena, which is the change of the resistance of a dielectric media by means of electric pulses.[4] The standard ReRAM cell is a capacitor-like structure in which the active material is placed in between two metal electrodes. Depending on the specific materials and its configuration, the resistive switching can be an interfacial effect (i.e., occurring in the proximity of the electrodes) or a bulk effect. In general, when the RS is interfacial, the cell is designed to have only one switching interface. Nevertheless, configurations with two ReRAM cells in series or two switching interfaces are arising because they hold notable technological advantages when integrated in large crossbar-arrays.[5]

In this work, we study metal-semiconductor-metal HfO_{2-x}-based devices where both interfaces display bipolar resistive switching, i.e., the resistance of each metal-HfO_{2-x} interface can be switched between a high-resistance state (HRS) and a low-resistance state (LRS) by applying electric pulses. The bipolar character of the RS means that the SET process (switch from HRS to LRS) and the RESET process (switch back from LRS to HRS) occur at opposite bias. In the literature, this configuration was reported as a "switchable rectifier",[6] and in a more general context, it belongs to the family of devices that presents complementary resistive switching.[5,7–9] Due to the non-linear character of the resistive switching phenomena, the configuration in series of two switching interfaces leads to nontrivial electrical characteristics; for example, hysteretic I–V (current-voltage) curves that differ from the typical self-crossing curves found in most of the RS devices.[10] In some systems, it is possible to include extra electrodes in order to monitor the contribution of each interface separately,[8] but when this alternative is not possible, the electrical characteristics are rationalized by comparing the behavior of a connection in series of two individual devices containing one switching interface,[5,9,11,12] or by mathematically modeling the system.[13,14] Here, we use an analysis method based on hysteresis switching loops (HSLs) that allows us to individuate the role of each interface and to model the switching mechanism. The understanding of the individual interfaces allows us to mathematically reproduce the behavior of the whole device and to understand the origin of the non-conventional I–V curves. Finally, we verify our procedure by changing the resistive switching character of only one of the interfaces.

We fabricated metal-semiconductor-metal HfO_{2-x}-based devices on Si/SiO_2 (150 nm) thermal oxide substrates on which the Ti bottom electrode (20 nm) was sputtered. The subsequent HfO_2 layer (20 nm) was grown by means of atomic layer deposition (ALD) technique at 300 °C using H_2O as oxidant and Tetrakis(dimethylamino)hafnium (TDMAH) as hafnium precursor. Finally, an array (16×5) of 35 nm-thick Co/Pd top electrodes (200×200 μm^2) was produced by sputtering and photolithography. Electrical characterization was carried out at a probe station (room temperature) using a Keithley 2635A sourcemeter controlled by custom computer software.

In Figs. 1(a) and 1(b), we present a scheme of the experimental setup and a typical current (I)-voltage (V) curve obtained for a Ti/HfO_{2-x}/Co device. This curve does not correspond to the typical hysteresis loop expected in RS devices. Figs. 1(c) and 1(d) sketch the conceptual difference between the I–V characteristic of our device and, as a typical example, the I–V loop of a bipolar RS device (Ref. 10 contains a comprehensive classification of I–V curves in RS devices). In our devices, the two branches of the hysteresis loop do not intersect at zero voltage. Moreover, the resistance state sensed turns from LRS to HRS when the voltage polarity is reversed. This kind of non-intersecting curve is generally observed in systems with complementary RS interfaces.[5]

a)E-mail: pablo.stoliar@cnrs-imn.fr

In order to disentangle the contribution of each interface, HSLs at opposite bias voltages were conducted. HSL is a parametric plot that displays the evolution of the resistance of a RS device during the application of a train of electrical pulses.[15–17] Throughout this work, HSL plots are defined as the sequence of points ($V_{PULSE}(i)$, $R_{REM}(i, V_{READ})$), being i the pulse index, V_{PULSE} the voltage of the ith pulse and R_{REM} is the remnant resistance *after* the ith pulse, which is sensed with the reading voltage V_{READ}. Here, the polarity of this V_{READ} is crucial due to the rectifying character of the interfaces. At positive V_{READ}, the current flowing through the device is mainly limited by the Ti/HfO_{2-x} interface and the HfO_{2-x} layer; the other interface is in direct bias so that it presents a negligible resistance. Assuming that the HfO_{2-x} bulk does not modify its resistance, any effect observed in the HSL that is acquired with positive reading voltage, is attributed to resistive switching in the Ti/HfO_{2-x} interface. Complementary, the HSL obtained with negative V_{READ} reveals RS in the Co/HfO_{2-x} interface.

The HSL of Fig. 2(a) was obtained with positive $V_{READ} = 4\,V$ applying 20ms-width pulses with a sequence $0\,V \rightarrow 15\,V \rightarrow -5\,V \rightarrow 0\,V$ in steps of 100 mV. The data clearly corroborates the bipolar character of the resistive switching. It also shows that for the Ti/HfO_{2-x} interface the minimum SET voltage is ~5 V. Even if the RESET procedure starts at low voltages, pulses should overcome ~−3 V to ensure proper RESET. For negative $V_{READ} = -4\,V$, Fig. 2(b) evidences that the SET and RESET voltages of the Co/HfO_{2-x} interface are ~−10 V and ~3 V, respectively. From these HSLs, it is also evident that the interfaces are complementary, for example, a positive voltage SETs the Ti/HfO_{2-x} interface but RESETs the Co/HfO_{2-x} interface.

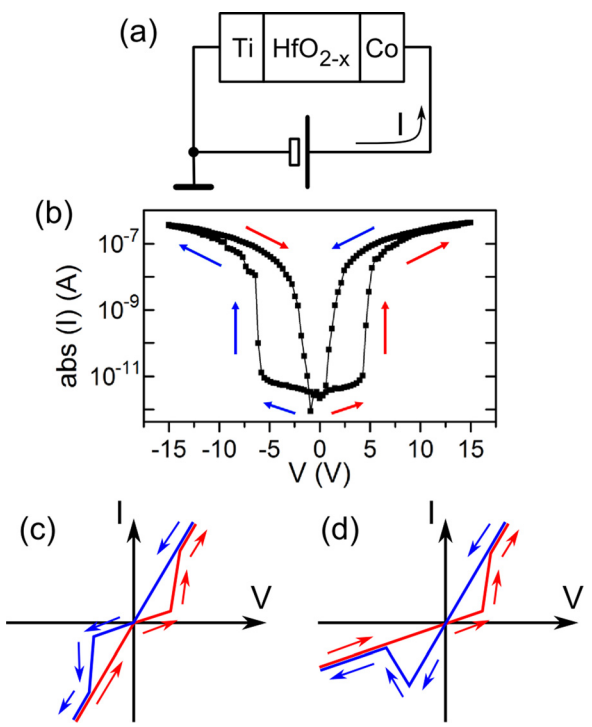

FIG. 1. (a) Schematic diagram of the experimental setup and (b) typical I–V curve of the Ti/Hf_{2-x}/Co devices. (c), (d) Schemas pointing out the radically different behavior observed in our devices (c) with respect to what is expected in standard bipolar RS devices (d). It implies a discontinuity in the resistance state when the polarity of the applied voltage changes.

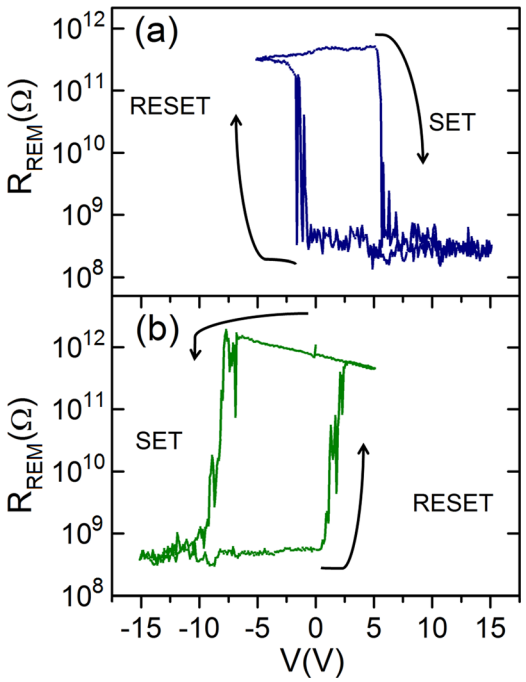

FIG. 2. Hysteresis switching loops obtained with opposite sensing bias on the same device. (a) When the sensing bias is +4 V, it reveals the behavior of the Ti/HfO_{2-x} interface. (b) Instead, when the bias is −4 V, it evidences the behavior of the Co/HfO_{2-x} interface.

The conceptual picture of these two complementary interfaces presenting bipolar resistive switching, confirmed by the HSLs, is schematized in Fig. 3. The device can be divided into (from left to right in Fig. 3(a)) a left contact (C_L), an interface region (I_L) modeled as a Schottky barrier, a bulk layer, and finally the interface region (I_R) corresponding to the right contact (C_R). The energy band diagram of the system in thermal equilibrium, assuming an n-type semiconductor, is presented in Fig. 3(b).[18] The RS mechanism found in our devices is attributed to local changes in the oxygen vacancy density at the interfaces by means of electric field. These changes result in a modification of the injection barriers, which in turn produces a modulation of their effective resistance. This mechanism has been widely reported for several systems,[11,19,20] as well as for HfO_{2-x}.[21–24] In fact, oxygen vacancies originate a sub-band at the HfO_{2-x} bandgap,[25,26] turning the Schottky barrier into an ohmic junction.[27] The SET process occurs when local electric fields increase the concentration of oxygen vacancies at the interfaces. The RESET process (at opposite polarity) removes the oxygen vacancies from the interfaces, restoring the original injection barrier. Typically, our device can display three different configurations, with only one of the interfaces in LRS (as in Figs. 3(c) and 3(d)) or with both interfaces in LRS (Fig. 3(e)). As we shall see later, a state with both interfaces in HRS is not recovered in normal operation.

We articulate the physical scenario described above into the following mathematical framework. The current flowing through the device, I, is modulated by the two interfaces (I_L and I_R, modeled as Schottky barriers) and the semiconducting bulk. The bulk is modeled as a linear resistor with

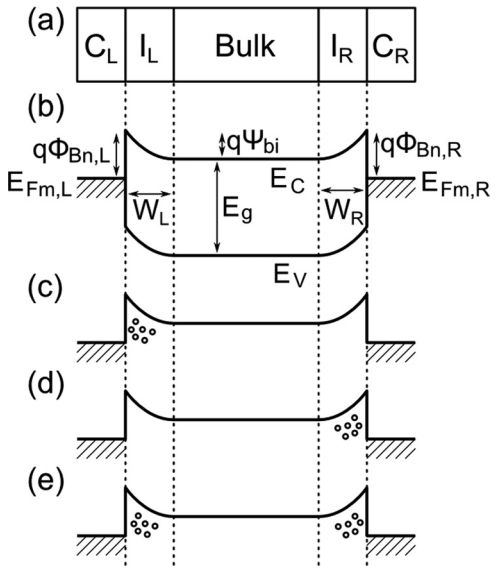

FIG. 3. (a) Schematic illustration of the structure of our devices. (b) Energy band diagram at thermal equilibrium of the system, where $E_{Fm,L}$ and $E_{Fm,R}$ are the Fermi energies of the metal contacts (C_L, C_R), W_L and W_R are the widths of the depletion layers, E_g is the energy band gap of the semiconductor, $q\psi_{bi}$ is the built-in potential, E_V and E_C are the valence and conduction band, respectively, and $q\Phi_{Bn,L}$ and $q\Phi_{Bn,R}$ are the energy heights of the Schottky barriers. (c–e) Different possible configuration of the system; with high concentration of oxygen vacancies (spheres) at the left interface (c), right (d), and in both interfaces (e). For the sake of simplicity, in this plot, we represented the injection barriers alike and not changing after the introduction of the oxygen vacancies. Actually, in our model, we assume that the injection barriers are strongly modified by the oxygen vacancies, turning the metal-semiconductor interfaces into ohmic contacts. We also account for unlike junctions.

constant resistivity, i.e., we consider non-linear effects only at the interfaces. The applied bias V is the sum of the voltage drop at each of the three components

$$V = -V_L(-I, n_L) + IR_B + V_R(I, n_R), \tag{1}$$

where $V_{L,R}$ are the potential drop at each interface, $n_{L,R}$ are the concentration of oxygen vacancies at the interfaces, and R_B is the resistance of the bulk region. The functions $V_{R,L}(I, n_{R,L})$ express the rectifying characteristics of the metal-semiconductor interfaces. Here, we assume that the transport through the interfaces can be captured by the thermionic-emission-diffusion model for conduction in metal-semiconductor interfaces[18]

$$V_{R,L} = \frac{k_B T}{q} \ln[1 + (I/i_0(n_{R,L}))], \tag{2}$$

where k_B is the Boltzmann constant, q is the carrier charge, T is the temperature, and i_0 is the saturation current. This assumption is based on the hypothesis that it is not possible to develop a stable large reverse voltage across the interfaces. In fact, as soon as the electric field increases, it activates the introduction of oxygen vacancies towards the interface, increasing the saturation current ($i_0 \propto n_{R,L}$).[18] The RS behavior is simulated as a modulation of the energy barriers by means of n_R and n_L

$$\frac{d}{dt} n_{R,L} = \mathrm{sgn}(V_{R,L}) \exp(-E_0 + |V_{R,L}/W_{R,L}|), \tag{3}$$

where E_0 is the anchoring energy of the oxygen vacancies to the HfO_{2-x} matrix and W_R and W_L are the depletion layer widths of the interfaces. The application of voltage pulses generates electric fields V_L/W_L and V_R/W_R strong enough to overcome the anchoring energy of the ions (see Ref. 13), triggering a redistribution of vacancies between the bulk and the interfaces. Whether the electric field introduces or removes ions from the interfaces depends on the polarity.

By numerical integration of Eq. (3), we obtain the temporal evolution of vacancy distributions at the interfaces, n_L and n_R. The integration must be performed in self-consistency with Eqs. (1) and (2), obtaining also the evolution of the device current, I, and the voltage drop at each interface for any applied voltage waveform $V(t)$.[28] In short, we can simulate the I–V characteristics and study the distribution V along the interfaces and the bulk. Fig. 4(a) shows the excellent agreement between experimental and simulated I–V curves for Ti/HfO_{2-x}/Co.

Here, we comment about the slight mismatch between the experimental data and the model. In the first place, both leak currents as well as the sensitivity of the SourceMeter prevent to measure currents below 1 pA, creating a mismatch between experimental data and simulation when the voltage approaches zero. The difference in the LRS is due to nonlinearities (see steps (3) and (6) in Fig. 4). The model considers that in the LRS the current is mainly limited by the linear bulk resistance. Instead, the experimental data presents a nonlinear behavior. This effect might rise from nonlinearities in the bulk I–V characteristics and/or from a non-negligibly influence of the injection barriers. Finally, a key point is that the model is not considering the profile of the vacancies at the interface; instead the interface is represented with a concentrated parameter model. We think this might be the reason behind the differences between the simulated and experimental data during the SET processes (see steps (2) and (5) in Fig. 4).

The evolution of these simulated parameters is crucial for the interpretation of the I–V curve, which is described in Figs. 4(b)–4(d). The current in the first quadrant of the I–V loop (positive bias) is governed by the Ti/HfO_{2-x} interface (I_L) and the bulk, whereas it is dictated by the HfO_{2-x}/Co interface (I_R) and the bulk in the third quadrant (negative bias). We can only infer the behavior of the "hidden" interfaces with the aid of the numerical simulations. The different states of the system are numbered in a sequence from (1) to (6) in both Figs. 4(a) and 4(d). We start our analysis with the Ti/HfO_{2-x} interface in HRS (almost free of oxygen vacancies) and the HfO_{2-x}/Co interface in LRS (with a high concentration of vacancies), corresponding to (1). Initially, almost all the electrical potential drops in the Ti/HfO_{2-x} interface, which is the main limitation for the current. When the voltage reaches the SET voltage of the Ti/HfO_{2-x} interface (2), it switches to the LRS. This SET voltage can be observed in the HSL presented in Fig. 2(a). Subsequently, the applied voltage turns to drop mainly at the bulk, which is now the limiting factor for the current. Some electric field also develops at the HfO_{2-x}/Co interface that RESETs (3). Nevertheless, the RESET of this interface has no effect in the current as long as the device is biased with positive voltage (4). The interface can be observed in the HSL in

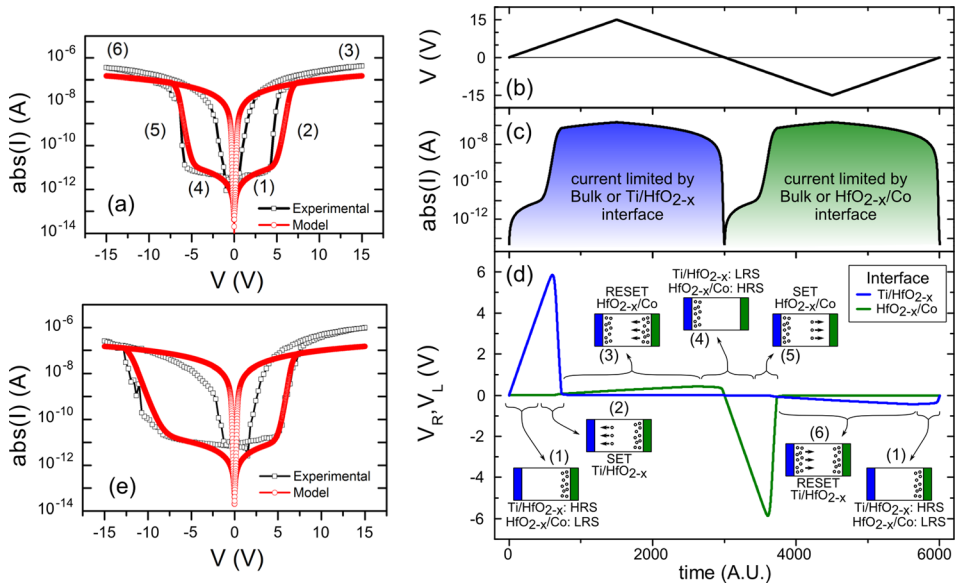

FIG. 4. Experimental and simulated I–V curves for the devices Co/HfO_{2-x}/Ti (a) and Au/HfO_{2-x}/Ti (e). (b–d) Evolution of the simulated parameters in time-steps, corresponding to the numerical integration presented in (a). For positive bias (voltage is presented in panel (b)), the HfO_{2-x}/Co interface do not limit the injection of carriers into the device, the current is governed by the Ti/HfO_{2-x} interface and the bulk; for negative bias it is limited by the HfO_{2-x}/Co interface and the bulk (see panel (c)). The sequence of the different states of the system is presented in panel (d) together with the voltage at the interfaces. This sequence, numbered (1) to (6) in accordance with panel (a), is: (1) the Ti/HfO_{2-x} interface is in HRS and the HfO_{2-x}/Co interface is in LRS, (2) SET of the Ti/HfO_{2-x} interface, (3) RESET of the HfO_{2-x}/Co interface, (4) state complementary to (1), (5) the SET of the HfO_{2-x}/Co interface, and finally (6) RESET of the Ti/HfO_{2-x} interface.

Fig. 2(b). When the bias polarity is reversed to negative values, the I–V reveals the HRS of the HfO_{2-x}/Co interface. In this quadrant, the SET of the HfO_{2-x}/Co interface is clearly reflected (5), but not the subsequent RESET of the Ti/HfO_{2-x} interface (6). Essentially, for negative bias, the HfO_{2-x}/Co interface limits the current until it SETs and then the current is dominated by the bulk. As mentioned, a state with both interfaces in HRS is not present in normal operation conditions.[29]

We finally consider a non-trivial confirmation of the whole model, testing it in devices with configuration Ti/HfO_{2-x}/Au, i.e., we substituted the Co electrode by Au. The rationale behind this substitution lies in the marked difference in the enthalpy of these two metals to react with an HfO_2 matrix.[30] The modification of the I_R should mainly impact on the third quadrant (negative bias) and indeed it creates a marked asymmetry in the I–V characteristics (Fig. 4(e)). As predicted, positive bias senses the state of the Ti/HfO_{2-x} interface (I_L) while negative bias senses the HfO_{2-x}/Au interface (I_R). Moreover, Fig. 4(e) presents the perfect agreement when we introduce an asymmetry in the widths of the depletion layers $W_R = 3\ W_L$ in Eq. (3). This is consistent with a picture in which a "textbook" Schottky barrier is formed at I_R when the Au electrode is in contact with the semiconductive layer. In contrast, the higher reactivity of the Ti effectively reduces the extension of the barrier.[19]

In conclusion, we fabricated and studied the resistive switching characteristics of metal-semiconductor-metal HfO_{2-x}-based devices presenting a particular non-crossing hysteresis loop. We proposed and validated the use of hysteresis switching loop with opposite sensing bias in order to disentangle the contribution of each interface. In that way, we confirm that both interfaces display bipolar resistive switching. In fact, they commute between a HRS, due to the injection barrier of the metal-semiconductor interface, and a LRS caused by an accumulation of oxygen vacancies that turns the interface into an ohmic contact. Moreover, at relatively high voltages (~10 V) the interfaces eventually complement each other, so that if one is at HRS the other one is at LRS. Based on this description, we were able to mathematically study the interplay between both switching interfaces, and more importantly, to rationalize the particular behavior observed in the I–V curves. Finally, we confirmed the validity of all the procedure by verifying the prediction that each interface is univocally related to a specific quadrant on the I–V hysteresis loop.

The authors acknowledge P. Levy for useful discussions. This work was supported by the project MAT2009-08494 and MAT2012-37638 from the Spanish Ministry of Science, by the Basque Government through the Project No. PI2011-1 and by the Marie Curie Reintegration Grant (ITAMOSCINOM) from the European Commission. F.G. is a member of CONICET.

[1]A. Sawa, Mater. Today **11**, 28–36 (2008).
[2]D. S. Jeong, R. Thomas, R. S. Katiyar, J. F. Scott, H. Kohlstedt, A. Petraru, and C. S. Hwang, Rep. Prog. Phys. **75**, 076502 (2012).
[3]R. Waser and M. Aono, Nature Mater. **6**, 833–840 (2007).
[4]M. Rozenberg, Scholarpedia J. **6**, 11414 (2011).
[5]E. Linn, R. Rosezin, C. Kügeler, and R. Waser, Nature Mater. **9**, 403–406 (2010).
[6]H. Shima, N. Zhong, and H. Akinaga, Appl. Phys. Lett. **94**, 082905 (2009).
[7]D. B. Strukov and H. Kohlstedt, MRS Bull. **37**, 108–114 (2012).
[8]M. Quintero, P. Levy, A. G. Leyva, and M. J. Rozenberg, Phys. Rev. Lett. **98**, 116601 (2007).
[9]M.-J. Lee, C. B. Lee, D. Lee, S. R. Lee, M. Chang, J. H. Hur, Y.-B. Kim, C.-J. Kim, D. H. Seo, S. Seo, U.-I. Chung, I.-K. Yoo, and K. Kim, Nature Mater. **10**, 625–630 (2011).

[10]J. J. Yang, I. H. Inoue, T. Mikolajick, and C. S. Hwang, MRS Bull. **37**, 131–137 (2012).
[11]J. J. Yang, M. D. Pickett, X. Li, D. A. A. Ohlberg, D. R. Stewart, and R. S. Williams, Nat. Nanotechnol. **3**, 429–433 (2008).
[12]A. Shih, W. Zhou, J. Qiu, H. J. Yang, S. Chen, Z. Mi, and I. Shih, Nanotechnology **21**, 125201 (2010).
[13]M. J. Rozenberg, M. J. Sanchez, R. Weht, C. Acha, F. Gomez-Marlasca, and P. Levy, Phys. Rev. B **81**, 115101 (2010).
[14]D. S. Jeong, H. Schroeder, and R. Waser, Nanotechnology **20**, 375201 (2009).
[15]Y. B. Nian, J. Strozier, N. J. Wu, X. Chen, and A. Ignatiev, Phys. Rev. Lett. **98**, 146403 (2007).
[16]M. Ungureanu, R. Zazpe, F. Golmar, P. Stoliar, R. Llopis, F. Casanova, and L. E. Hueso, Adv. Mater. **24**, 2496–2500 (2012).
[17]F. Gomez-Marlasca, N. Ghenzi, M. J. Rozenberg, and P. Levy, Appl. Phys. Lett. **98**, 042901 (2011).
[18]S. M. Sze and K. K. Ng, *Physics of Semiconductor Devices*, 3rd ed. (Wiley-Interscience, New York, 2007).
[19]A. Sawa, T. Fujii, M. Kawasaki, and Y. Tokura, Appl. Phys. Lett. **85**, 4073–4075 (2004).
[20]N. Ghenzi, M. J. Sanchez, F. Gomez-Marlasca, P. Levy, and M. J. Rozenberg, J. Appl. Phys. **107**, 093719 (2010).
[21]M. Y. Chan, T. Zhang, V. Ho, and P. S. Lee, Microelectron. Eng. **85**, 2420–2424 (2008).
[22]P. Gonon, M. Mougenot, C. Vallee, C. Jorel, V. Jousseaume, H. Grampeix, and F. El Kamel, J. Appl. Phys. **107**, 074507 (2010).
[23]H. Y. Lee, P. S. Chen, T. Y. Wu, Y. S. Chen, C. C. Wang, P. J. Tzeng, C. H. Lin, F. Chen, C. H. Lien, and M.-J. Tsai, in *Electron Devices Meeting, 2008. IEDM, IEEE International* (IEEE, 2008), pp. 1-4.
[24]H. Y. Lee, Y. S. Chen, P. S. Chen, T. Y. Wu, F. Chen, C. C. Wang, P. J. Tzeng, M. J. Tsai, and C. Lien, IEEE Electron Device Lett. **31**, 44–46 (2010).
[25]K. Xiong, J. Robertson, M. C. Gibson, and S. J. Clark, Appl. Phys. Lett. **87**, 183505 (2005).
[26]X. Wu, D. B. Migas, X. Li, M. Bosman, N. Raghavan, V. E. Borisenko, and K. L. Pey, Appl. Phys. Lett. **96**, 172901 (2010).
[27]S. D. Ha and S. Ramanathan, J. Appl. Phys. **110**, 071101 (2011).
[28]See supplementary material at http://dx.doi.org/10.1063/1.4818730 for details on the numerical simulations.
[29]We observe that both interfaces are in HRS in pristine devices, i.e., new devices (as fabricated) exhibit HRS independently of the voltage bias polarity. Our devices do not require a standard forming procedure, and hence the voltage required to trigger the first HRS to LRS transition is basically the same than all the subsequent SET voltages. For positive voltages the electric field mainly develops at the Ti/HfO_{2-x} interface, independently of the state of the other interface (than can be either in HRS or in LRS).
[30]C. Vallée, P. Gonon, C. Jorel, and F. El Kamel, Appl. Phys. Lett. **96**, 233504 (2010).